Integration of Reservoir Simulation in Analysis Workflow

In this Part 3 of the paper installment, we continue discussion/analysis of the gas well surveillance data example presented in Part 2. In Part 2 we demonstrated analysis of this surveillance data using capabilities of the analysis module which is a core of Convolution Explorer application. In fact, Convolution Explorer has two modules: (1) analysis module, and (2) simulation module called Response Generator.

Response Generator is a reservoir simulation functionality that is closely integrated with the analysis module. Response Generator is a 2-D single-phase reservoir simulator. This is not a finite-difference or finite-element type simulator as majority of reservoir simulators used in the industry. It does not use areal gridding when solving fluid flow problems in the reservoir. It is based on a numerical boundary element solution algorithm but also includes some analytical elements like solving the problem in Laplace space instead of time domain and using numerical inversion algorithm to bring solution back to the time domain. It accurately predicts pressure behavior at the well locations that can be directly compared with the pressure measured by the pressure gauges located at the same well locations. This comparison can be done on a variety of plots (including derivative type plots) used in PTA analysis. This simulator allows interactively build reservoir models that honor true reservoir geometry and use reservoir descriptions consistent with the information content of analyzed pressure data. Using this simulation functionality alongside analysis module adds to the level of confidence that the analysis results and the conclusion of the analysis are sufficiently accurate and reliable. It also allows to develop some additional insights into reservoir dynamic behavior reflected in the observed surveillance data.

The 2-D single-phase reservoir simulator in Convolution Explorer is used only for computation of unit-rate drawdown pressure responses (both self-responses and interference responses) for each well. This is why within Convolution Explorer application this simulator is named Response Generator. After all simulated response functions are computed, they are then convolved with well rates using the same multi-well convolution algorithm used by analysis module. This convolution produces simulated well pressure at each well location. Note that Response Generator also uses linear approximation of fluid flow problem in the reservoir i.e., it is completely consistent with the assumptions and the limitation of PTA analysis approach.

Recap of Analysis, Results, and Conclusions from Part 2

As was discussed In Part 2, the example presents analysis of surveillance data from an offshore dry gas reservoir developed with three wells. The analyzed surveillance data came from a well completed in a separate fault block. It was not clear if this fault block is in pressure communication with the rest of the reservoir or not. There is also a possibility that this fault block could be connected to aquifer.

The analysis was based on the following input data:

1. Tables of gas properties (gas z-factor, gas compressibility, gas viscosity, gas pseudo-pressure) defined as functions of pressure
2. Several constant parameters that define rock properties (rock porosity, water saturation, rock compressibility, initial reservoir pressure. It is assumed that these values are applicable to entire reservoir.
3. Well Surveillance pressure and rate data defined as functions of time. These are data obtained during five-year production history of the well.

Summary of Results and Conclusions:

1. Single well analysis of surveillance data confirmed that this is indeed a separate fault block not communicating with the rest of the reservoir. Also, there is no evidence of aquifer pressure support reflected in this surveillance data.
2. Comparison of pressure transient behavior during a sequence of pressure buildups selected through the production history of the well shows reasonably consistent transient behavior throughout the entire 5-year history of well production. This data consistency evaluation also shows that the well skin factor decreases together with the well rate as a result of pressure depletion in the compartment drained by the well. This is an indication that the decreasing part of the skin factor is a turbulence rate-dependent skin component characteristic of high-rate gas wells.
3. Reconstruction of unit rate drawdown response of the well using specialized analysis workflow implemented in Convolution Explorer produced a response function which represents characteristic pressure behavior of the well during entire time span of well production history. This response reconstruction also produced an estimate of the reservoir pore volume of 255 mmRb.
4. Uncertainty assessment of the reconstructed drawdown response indicates that the response function is reasonably well defined by surveillance data. This provides confidence that further analysis that relies on reconstructed response function provides accurate and reliable estimates of reservoir and well characteristics.
5. Analysis of the reconstructed response function provides us with an estimate of formation average permeability in close proximity of the well (within the radius of 170 ft from the well). Reconstruction process of the response function produced an estimate of total pore volume of reservoir compartment drained by the well. It also tells us that the well is located close to the compartment boundary located about 170 ft from the well. The reservoir compartment is narrow and long (channel-type). The width of the channel is close to 1300 ft.

The most surprising and remarkable about pressure transient analysis approach is that it translates reservoir dynamic behavior (evolution of pressure and rate in time), recorded at just one location in the reservoir – at the wellbore, into a characterization/description of our reservoir as an object in space.

Incorporation of Geologic and Seismic Information into Analysis

So far, our investigation was limited to working with dynamic pressure and rate data acquired at the well location downhole. Well pressure and rate data are temporal data, but through the use of pressure transient analysis techniques these data reveal some information about the reservoir drained by our well. These are not just some reservoir characteristics, but they also define a picture of our reservoir, its image in space. This is not a clear picture; we cannot see or tell much about the true reservoir shape. The only thing we know is that the reservoir areally looks like a channel (narrow and long) with the width of the reservoir of around 1300 ft. However, we do have one piece of reservoir information that is reasonably well defined. It is the reservoir pore volume. In our case this volume is close to 255 mmRb.

Much better and more detailed pictures of reservoirs are derived from seismic and geologic data obtained in the course of reservoir appraisal. These data are eventually presented in the form of reservoir maps. However, these maps, while presenting a more detailed and clearer reservoir image in terms of spatial arrangement, are based on static data (geologic and seismic data). A map does not describe how a reservoir is plumbed together. Understanding of reservoir plumbing can come only from reservoir dynamic analysis. This leads us to a need of closer integration of our dynamic analysis with reservoir static description in the form of reservoir maps. The way to achieve such integration is through incorporation of reservoir simulation into our dynamic analysis workflow.

This is a right moment to present a map of our reservoir and to determine to what extent this map supports the analysis results derived from dynamic analysis. **Fig. 1** is the map of our reservoir. The red solid line defines the area of the reservoir. The map also presents locations of three wells drilled in this reservoir.

The map shows a number of faults running along the reservoir structure. Most of these faults are short and they should not impede communication across the field. There is, however, one major fault that on the map runs through most of the reservoir length. In case if it does not end as shown on the map but extends all the way to the reservoir south boundary, this fault could cut off a strip of the reservoir structure into a separate fault block. From our dynamic analysis we already know that this is indeed the case. The fault block is indeed a long and narrow channel-like strip of the structure as indicated by our analysis. One of the reservoir wells is placed within this fault block. This is the well that is the subject of our analysis. The map shows that this well is located close to the fault that cuts off the fault block from the rest of the reservoir. This is another confirmation of consistency of our analysis results with the reservoir map.

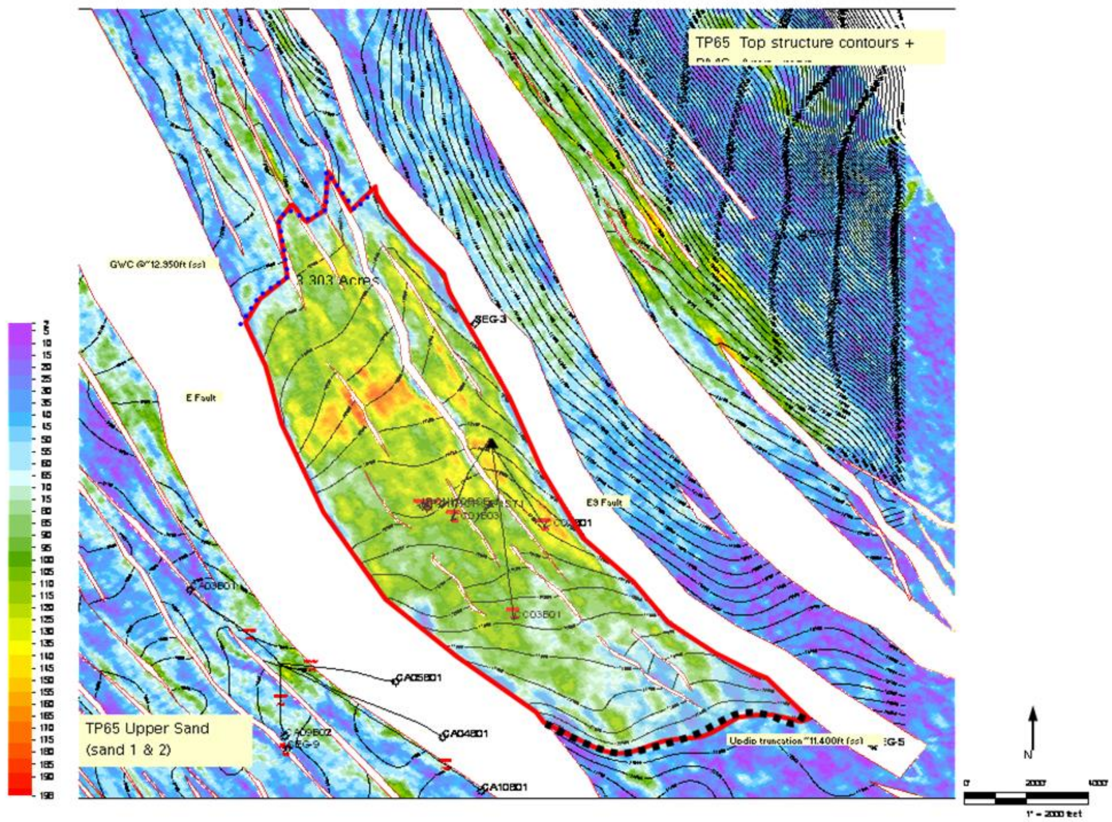

Fig . 1. Reservoir map.

Simulation Reservoir Model

In the context of reservoir analysis workflow, we resort to reservoir simulation not as a way to build a reservoir model that matches observed surveillance data. This is not the objective here. We look at reservoir simulation as a way to bring reservoir map (geologic and seismic information) into analysis workflow in order to gain some additional insights into observed dynamic behavior and whether this behavior is consistent with the available static reservoir description in the form of a reservoir map.

Here we present a reservoir model that is used by Response Generator to solve fluid flow equations and simulate the flow in the reservoir that occurs in the course of production. Fluid flow simulation is performed using the same well rate history, the gas and rock properties as that used in the analysis discussed in the Part 2 of this paper. Rock properties in the model are constant throughout the entire reservoir area. In addition to static rock properties, we have to specify the permeability of reservoir formation. This permeability is set equal to the permeability estimate obtained in the dynamic analysis. Again, we assume that this permeability is constant throughout the reservoir area.

The reservoir boundary in the model is defined according to the reservoir map. One of the boundaries in this model runs along the fault that separates the fault block from the rest of the reservoir. We have the problem here because it is not clear how to extend this boundary all the way to the south edge of the reservoir. There are two short faults shown on the map in this area. It is likely that one of these short faults is actually the extension of the separation fault to the south reservoir boundary. In deciding which of these short faults to choose, we use the information about the pore volume of the reservoir compartment drained by the well. We experimented with these two possible scenarios for fault extension and ended up with the reservoir boundary shown in **Fig. 2**.

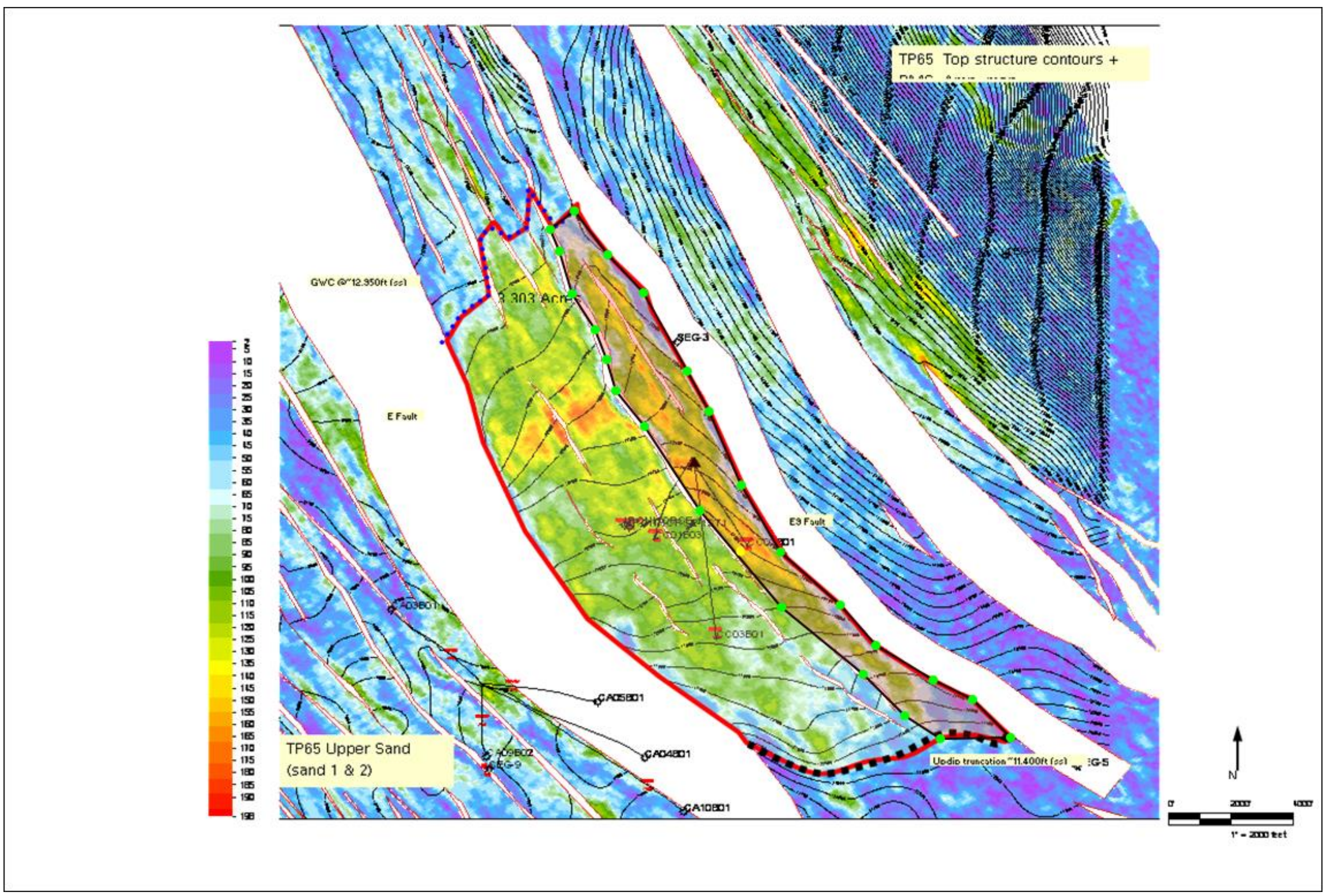

Fig. 2. Reservoir model. The model boundary is defined by black solid line segments connecting control points (shown in green) that are used to define the shape of reservoir boundary. The yellow point marks the well location in the model.

The reservoir boundary in **Fig. 2** is presented as a polygon. Polygon vertices are shown as green points. These points are distributed along the reservoir fault block boundary as shown on the map. The polygon vertices are connected by black solid line segments that together define the reservoir boundary in the model.

The reservoir rock properties used in the model are presented in the tables in **Fig. 3**. The first table presents rock properties. The second table presents summary data about the model as a whole. This information includes the area, the pore volume, and the volume of gas initially in place in the model. Note that the model pore volume (259.8 mmRb) is slightly higher but very close to the pore volume value (255 mmRb) derived in the analysis.

Index	Poly Name	Perm, md	Por, frac	Sw, frac	H, ft	Cr, 1/psi
0	A	72.6	0.18	0.29	255	5.7E-06

Name	Area, acre	Pore Volume, mmRB	HIIP, Bcf
A	729.52	259.7875	313.3942
pn-C1	729.52	259.7875	313.3942

Fig. 3. The rock properties used in the model. The first table presents rock properties and the second provides summary information about the model.

Consistency of Reservoir Dynamic Analysis Results with Static Reservoir Description Reflected in Reservoir Map

Before we proceed with discussion of simulation results and compare them with what we did earlier in reservoir dynamic analysis (discussed in Part 2 of the series) it is instructive to review the two components of the overall workflow.

In the analysis step we **do not** build a reservoir model; we **do not** simulate fluid flow in the reservoir. We interactively reconstruct the unit-rate drawdown response function; on each step of this reconstruction process we convolve the current response function with the well rate and compare the result of convolution with appropriately selected portions of observed pressure data. We stop this process after the necessary match is achieved. We do all this without any prior knowledge of the reservoir, its map, and its properties. The only constraint that limits/guides our actions is the requirement to produce a constant rate drawdown response that we consider as "physically meaningful".

In the simulation step of the analysis workflow, we build a reservoir model based on prior reservoir information reflected in the reservoir map and some reservoir characteristics already derived in the above analysis step (reservoir permeability, reservoir pore volume). We then run

Response Generator (simulator) and compute simulated response. Next, we convolve this simulated drawdown response with the well rate and compute simulated pressure during the entire production history of the well. In this step of the workflow, simulation results are constrained by the reservoir model, reservoir geometry, reservoir properties. It is not obvious that the two sets of results will be consistent. In the first approach, we assume that observed pressure data reflect the **true reservoir as it exists insitu** underground and draw conclusions about the properties of this reservoir. In the second simulation approach we rely on the reservoir model which is defined based **on our understanding** of the reservoir properties, reservoir shape, size and so on. Our understanding of the reservoir may be correct, or it may be wrong. Hence, the two sets of results can only be consistent if the reservoir model used in simulation correctly represents the reservoir as it exists underground.

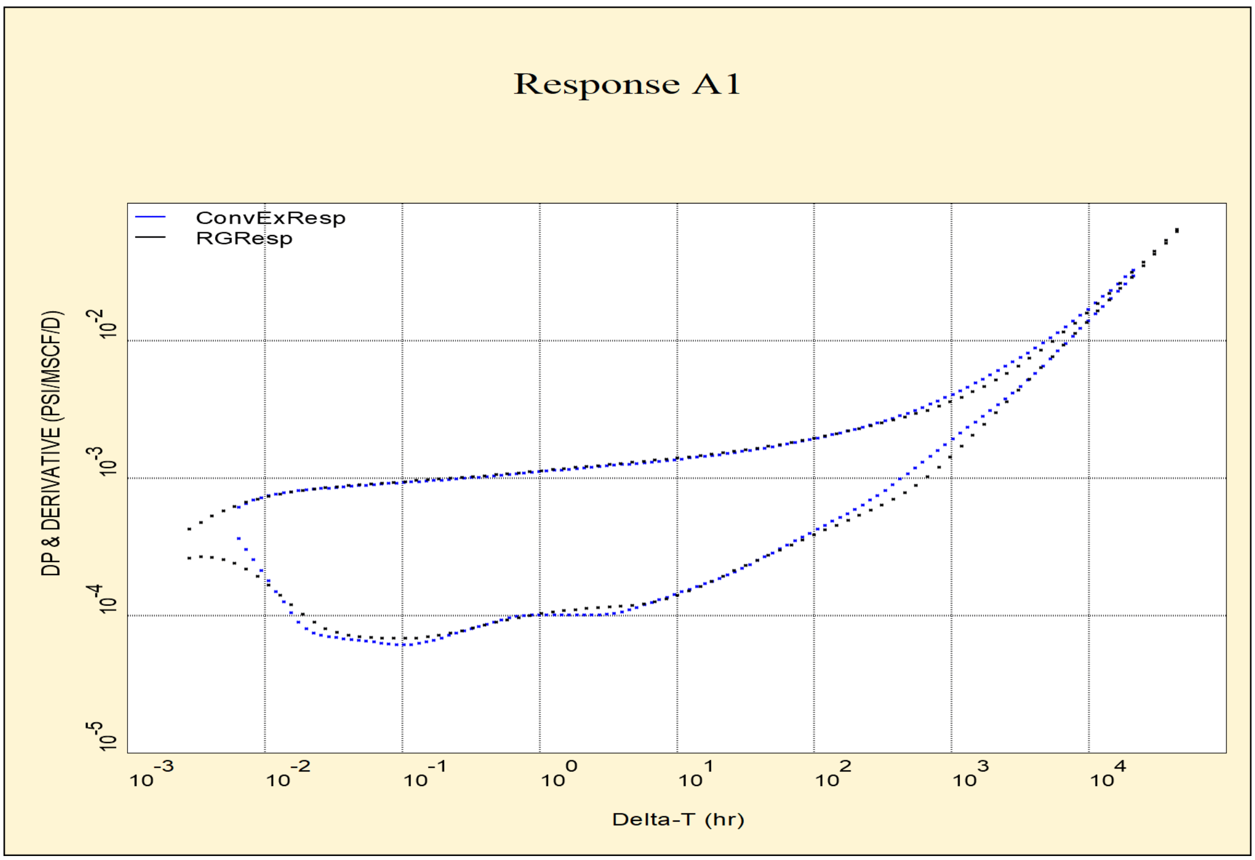

Fig. 4. Comparison of reconstructed and simulated unit-rate drawdown responses.

After this comparative review we proceed now with comparison of simulation result with the results derived in the analysis step. **Fig. 4** compares a response derived in the analysis step through response reconstruction (dark blue) and the response produced by Response Generator. The two responses are reasonably consistent. They honor the features of transient behavior at early time and also reflect essentially the same value of reservoir pore volume that controls the unit-slope asymptotic trend at late time. There is some level of mismatch of the two responses during the time interval from 150 hrs. through 2000 hrs. This mismatch is an indication that our reservoir model does not accurately reflect the true properties of the reservoir. This mismatch of responses in **Fig. 4** points us to a conclusion that it is likely caused by variation of reservoir properties across the reservoir. Recall that the model assumes the reservoir properties homogeneous throughout the reservoir area. There are probably multiple ways to adjust the reservoir description in the model to improve the match. This is a common problem with reservoir simulation approach – it does not lead to sufficiently unique result when simulation is used in the context of inverse problem solution.

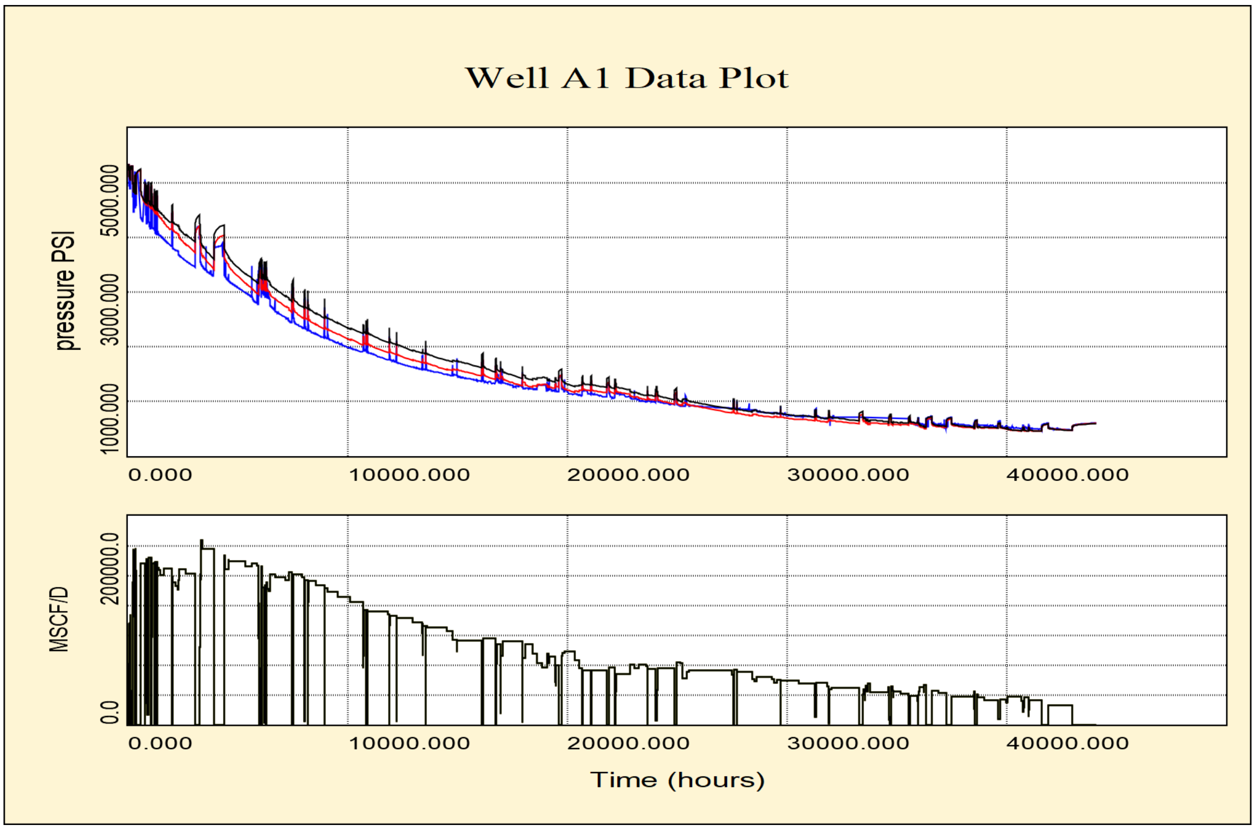

Fig. 5. Simulated pressure behavior vs. the pressure prediction based on the reconstructed pressure response.

Fig. 5 compares the simulated well pressure (black), the well pressure computed by convolution of reconstructed drawdown response with well rate (red), and the observed well pressure (blue). Note that the first two pressure functions do not take into account variation of well skin factor caused by turbulence effect. As a result, they do not reproduce the observed pressure (blue) during flow periods. Also, during a time period that starts soon after the start of production and extends through the first 20000 hrs. the simulated pressure curve is shifted slightly up compared to the convolved pressure prediction derived in the analysis step. This upward shift is the result of the responses mismatch in **Fig. 4**. If we adjust the reservoir model and eliminate the response mismatch in **Fig. 4** this will also bring the simulated pressure curve in **Fig. 5** down so that it matches the red curve.

Note, that the reservoir map in **Fig. 1** also suggests that the reservoir properties are not homogeneous and likely change throughout the reservoir area as indicated by the color attributes shown on the map. These color attributes result from seismic data interpretation.

Next, we demonstrate that the mismatch seen in **Fig. 4** and **Fig. 5** can indeed be eliminated by introducing permeability heterogeneities in our reservoir model. **Fig. 6** presents a slightly modified version of the model that has the same outer boundary, the same reservoir area and volumetric characteristics. However, the model area in this model is split into four polygon regions. The solid red lines define the interfaces between the polygons. At the same time these interface lines serve as connections between the polygons. Gas can freely flow from one region to the next across these polygon interface lines.

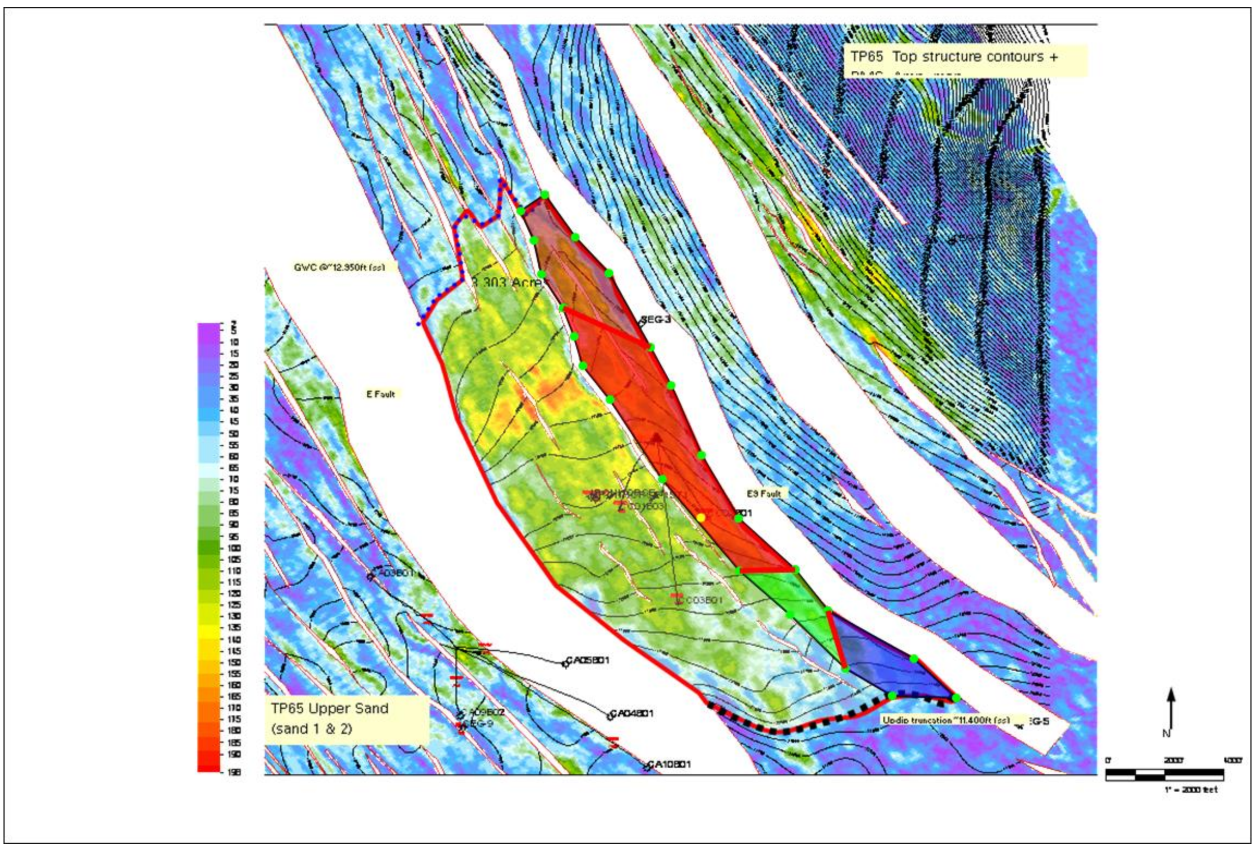

Fig. 6. Four-region reservoir model. The three red solid lines in the plot split the reservoir area into four polygon regions.

Fig. 7 presents the rock properties of the four regions in the model. Please note that porosity, water saturation, net thickness and rock compressibility are the same in each of the regions and are equal to the respective values used in the previous model. Only permeability changes between regions. The region named AB is the region where the well is located. The permeability in this region is the same as in the earlier model. The other three regions in the model have lower permeabilities.

Index	Poly Name	Perm, md	Por, frac	Sw, frac	H, ft	Cr, 1/psi
0	AB	72.6	0.18	0.29	255	5.7E-06
1	ABA	20	0.18	0.29	255	5.7E-06
2	ABAA	5	0.18	0.29	255	5.7E-06
3	ABB	5	0.18	0.29	255	5.7E-06

Fig. 7. Rock properties of the four-region reservoir model.

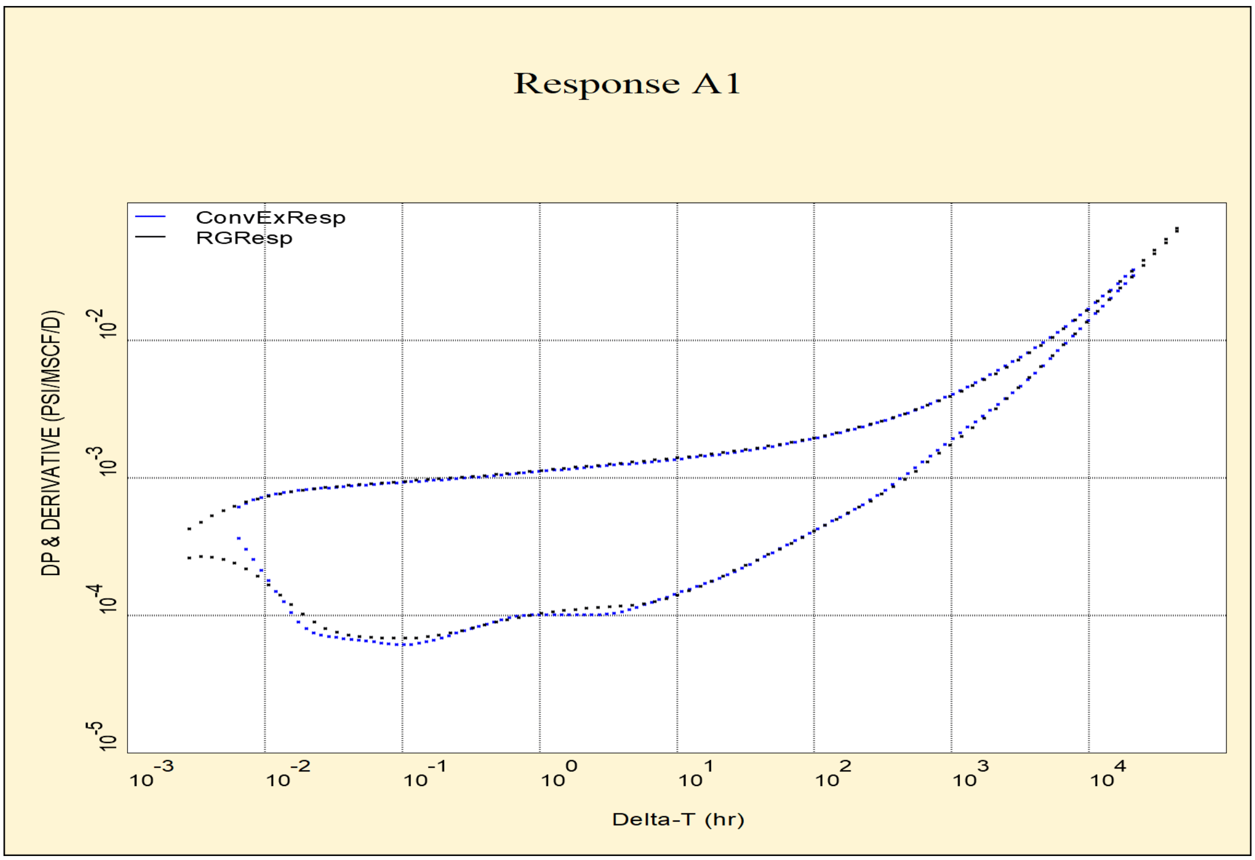

Fig. 8. Comparison of reconstructed and simulated unit-rate drawdown responses using four-region model.

The **Fig. 8** and **Fig. 9** below demonstrate that simulated response function and simulated pressure during the entire well production history match the drawdown response and the well pressure behavior derived in the Part 2 analysis very well now. This supports the notion that the observed dynamic reservoir behavior points to some form of heterogeneous rock properties in the reservoir.

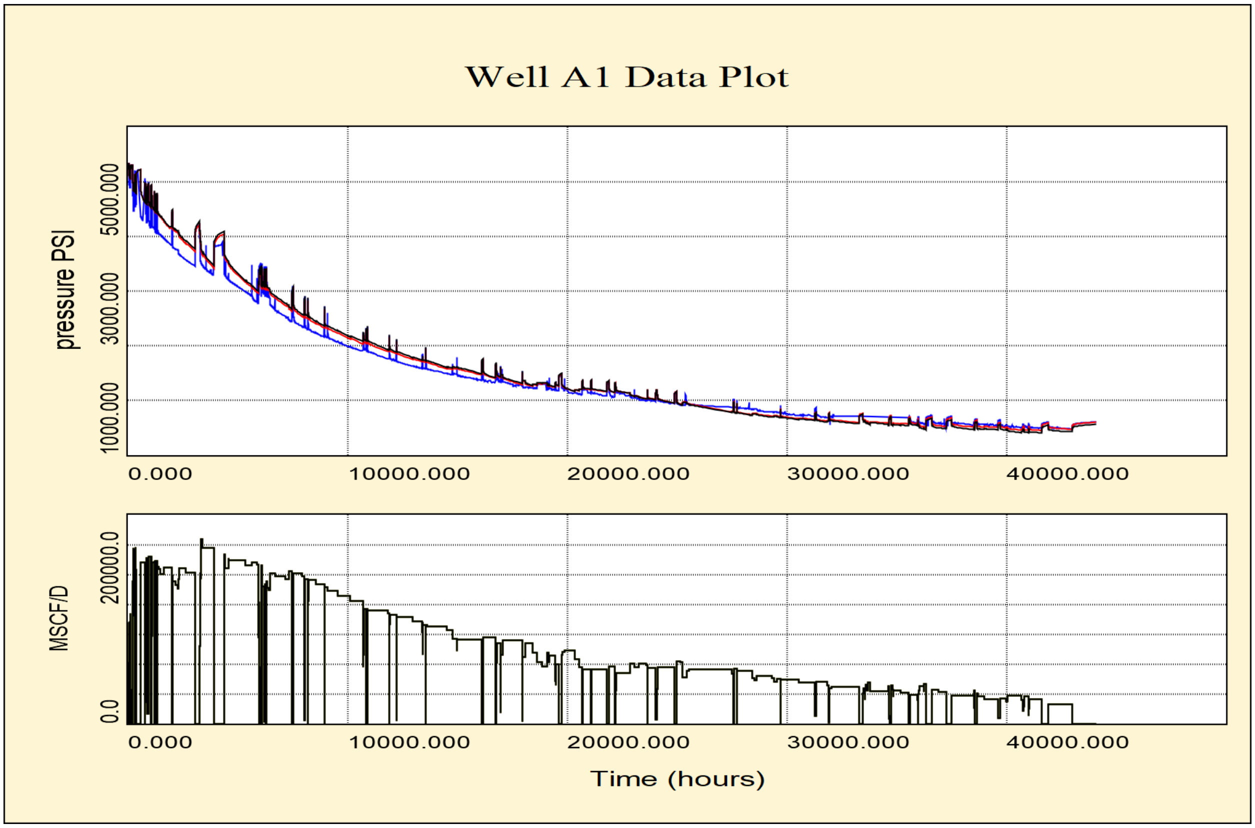

Fig. 9. Simulated pressure behavior based on the four-region model vs. the pressure prediction based on the reconstructed pressure response.

Summary

The discussion presented in this Part 3 of the series demonstrates that inclusion of simulation step into the overall reservoir dynamic analysis workflow is beneficial. It provides confidence that analysis results are consistent with additional reservoir information in the form of reservoir maps. The simulation step produces a simple reservoir model that is validated against observed dynamic reservoir behavior. Such model in itself may be useful. In our specific case this step provides an additional insight into the observed surveillance pressure behavior. It leads us to a conclusion that the observed well pressure behavior is affected by reservoir heterogeneities present in the reservoir.